Bull. Chem. Soc. Jpn., **77**, 1671–1679 (2004)

Natural Bond Orbital Analysis of Pericyclic and Pseudopericyclic 1,5-Electrocyclizations of Conjugated Nitrileimines

Kazuaki Fukushima* and Hideo Iwahashi

Wakayama Medical University, 811-1 Kimiidera, Wakayama 641-8509

Received January 5, 2004; E-mail: fuku@wakayama-med.ac.jp

Ab initio and DFT studies have revealed that there are three mechanisms in 1,5-electrocyclizations of conjugated nitrileimines. The first one is a pericyclic 1,5-electrocyclization of vinyl or (*Z*)-imino nitrileimine. Interactions between π-orbitals at C1 and X5 lead to formation of σC1–X5 bonds. The second one is a typical pseudopericyclic 1,5-electrocyclization of formyl nitrileimine. Nucleophilic interaction of lone pair electrons at O5 to π^*C1–N2(h) leads to formation of a σC1–O5 bond. The natural bond orbital (NBO) analysis for the reaction has shown that there are two disconnections of orbital interactions at C1 and O5 at the transition state because of the orthogonal array of the forming σC1–O5 bond and the other π-orbitals. The third one is an incomplete pseudopericyclic 1,5-electrocyclization of (*E*)-imino nitrileimine. Nucleophilic interactions of lone pair electrons at N5 to π^*C1–N2(h) and π^*C1–N2(v) lead to formation of a σC1–N5 bond. There is a single disconnection of orbital interactions at N5 at the transition state, because the forming σC1–N5 bond and the other π-orbitals are orthogonal at N5 but not at C1, owing to twisting in the nitrileimine moiety.

A pseudopericyclic reaction is one of the concerted reactions. The pseudopericyclic reaction is characterized by disconnections between orthogonally arrayed interacting orbitals, and is distinguished from pericylic reactions. The concept of a pseudopericyclic reaction is useful and widely applicable, although the original definition by Lemal et al. has some ambiguity.[1] Birney et al. have developed the concept and successfully applied it to cheletropic reactions, sigmatropic reactions, and cycloadditions.[2] They summarized the prominent features of the pseudopericyclic reactions as: (1) the reactions have low activation energy, (2) transition states of the reactions have planar geometry, and (3) the reactions cannot be symmetry forbidden.[2b]

Recently, several groups applied the concept of the pseudopericyclic reaction to electrocyclizations. In these reactions, substrates need to have orthogonally arrayed orbitals at both ends of the molecules. Thus, investigations have been concentrated to electrocyclizations of conjugated 1,3-dipoles of the propargyl-allenyl type (Fig. 1) and those of (*Z*)-1,2,4,6-heptatriene analogues.[3–8]

In the early work in this area, the existence of two types of transition states in 1,5-electrocyclizations of conjugated azides (**A**=**B**=**C**=N)[3] and diazomethanes (**A**=**B**=N, **C**=CH)[4] was pointed out without using the concept of the pericyclic and pseudopericyclic reactions. Extensive applications of the concept have been carried out for 1,5-electrocyclizations of conjugated nitrile ylides (**A**=**C**=CH, **B**=N) from various points of view.[5–7] Twisting of the conjugated groups and the nitrile ylide moiety is a remarkable stereochemical feature that differentiates pericyclic reactions from pseudopericyclic reactions.[5] In the reactions of vinyl (**D**=CH, **E**=CH$_2$) and (*Z*)-imino (**D**=CH, **E**=(*Z*)-NH) nitrile ylides, a vinyl group, an (*Z*)-imino group, and nitrile ylide moieties were twisted at the transition states, which showed that the reactions were disrotatory processes. In the reaction of (*E*)-imino (**D**=CH, **E**=(*E*)-NH) nitrile ylide, an (*E*)-imino group was not twisted at the transition state, and the geometry of the whole molecule was almost planar. In the reaction of formyl (**D**=CH, **E**=O) nitrile ylide, stereochemical information is not sufficient for determining reaction mechanisms, because the formyl group has no hydrogen atom on carbonyl oxygen. Calculated activation energies for the reactions of vinyl and (*Z*)-imino nitrile ylides were higher than those for the reactions of formyl and (*E*)-imino derivatives. According to Birney's criteria, the stereochemical features showed that the reactions of vinyl and (*Z*)-imino nitrile ylides are pericyclic reactions and that the reaction of (*E*)-imi-

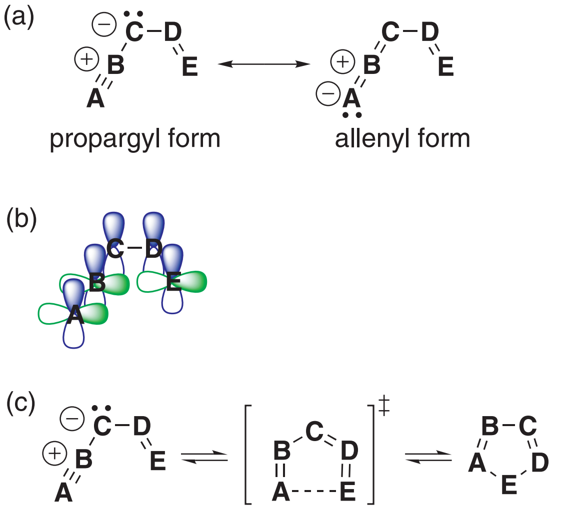

Fig. 1. (a) A Propargyl form and an allenyl form of conjugated 1,3-dipoles of the propargyl–allenyl type. (b) Orthogonal π-orbitals in conjugated 1,3-dipole of the propargyl–allenyl type. (c) 1,5-Electrocyclization of conjugated 1,3-dipole of the propargyl–allenyl type.

Published on the web September 10, 2004; DOI 10.1246/bcsj.77.1671

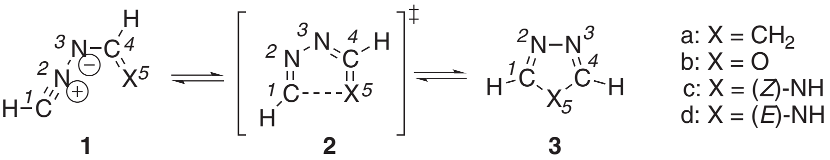

Fig. 2. General scheme of 1,5-electrocyclization and numbering system for conjugated nitrileimine (**1**), transition state (**2**), and the corresponding heterocycle (**3**).

no derivative is a pseudopericyclic reaction. The mechanism of the reaction of formyl nitrile ylide cannot be determined by stereochemical features only, but it seems to be a pseudopericyclic reaction because of the low activation energy. Such uncertainty in determination of the reaction mechanisms based on stereochemical and energetic features are serious problems in some electrocyclizations.

The pseudopericyclic and the pericyclic nature of the 1,5-electrocyclizations of the conjugated nitrile ylides have been confirmed by additional analytical methods of electronic properties. Rodriguez-Otero et al. reported magnetic properties of the reactions along intrinsic reaction coordinates (IRC).[6] The reactions of vinyl and (*Z*)-imino nitrile ylides showed minima of the magnetic susceptibilities and anisotropies at the transition states. This indicated that the transition states have an aromatic character. On the other hand, the reactions of (*E*)-imino and formyl nitrile ylides showed monotonous decreasing in the magnetic susceptibilities and anisotropies without any minimum, which can be interpreted as showing that the transition states of the reactions are not aromatic, which is characteristic in pseudopericyclic reactions.

In a previous paper, one of us reported analyses of the second order perturbative energy-lowering of donor/acceptor natural bond orbitals (NBOs) along IRC as an alternative analytical method for confirmation of the pseudopericyclic and the pericyclic nature in the 1,5-electrocyclizations of vinyl and formyl nitrile ylides.[7c] In the reaction of vinyl nitrile ylide, π–π^* interaction between C1 and C5 developed at the transition state. In the reaction of formyl nitrile ylide, however, n–π^* interaction between C1 and O5 developed at the transition state.

Nitrileimine (**A**=CH, **B**=**C**=N) is one of the propargyl–allenyl types of 1,3-dipoles (Fig. 2). The 1,5-electrocyclizations of the conjugated nitrileimines provide the corresponding five-membered heterocycles.[9,10] Lippmann et al. reported examples of typical reactivity of the conjugated nitrileimines.[11] They reported intramolecular competitive cyclizations of various conjugated groups and a 2-nitrophenyl group (Fig. 3). The nitro group predominantly cyclized to afford anthranil 1-oxide in the case where the conjugated group was C=C (path ***a***). On the other hand, when the conjugated group was C=O or C=N, it cyclized faster than the nitro group to afford oxadiazole or triazole derivative (path ***b***). At first glance, mechanisms of the 1,5-cyclizations of the conjugated nitrileimines seem to be the same as those of the conjugated nitrile ylides, because nitrileimines are analogues of nitrile ylides. However, conformations of some nitrileimine derivatives are different from those of nitrile ylides. Molecular orbital calculations showed that the structures of the nitrileimine moieties in some derivatives were almost linear forms.[12,13] In such derivatives, structural information on twisting in the nitrileimine moiety was lost. In this paper, we report ab initio and DFT calculations of the 1,5-electrocyclizations of conjugated nitrileimines, which are model compounds of the intramolecular competitive reactions. The lack of structural information has led us to apply the second order perturbation analysis of the NBO basis to determining the reaction mechanisms.

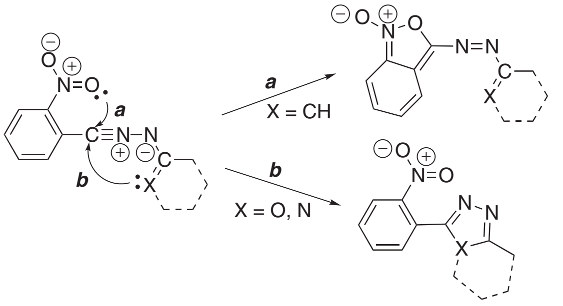

Fig. 3. Intramolecular competitive reactions of conjugated nitrileimines reported by Lippmann et al.[11]

Computational Methods

All calculations were carried out using Gaussian 98 W program.[14] Geometries were optimized using the MP2 level of theory[15] with the 6-31+G(d) and the 6-311+G(d,p) basis sets, and the B3LYP level[16] with the 6-311+G(d,p) basis set. All stationary points were characterized as minima or transition states by frequency calculations. The NBO analysis[17] was performed along IRC[18] at the MP2/6-31+G(d) level of theory.

Results and Discussion

Geometries and Energies. The geometry of nitrileimine is sensitive to the substituents and basis sets used.[12] We previously reported substituent-dependency of the geometries of conjugated nitrileimines.[13] The geometries of unsubstituted and conjugated nitrileimines optimized at the MP2/6-31G* level were bent forms with H1–C1–N2 angles of 140.9°–157.4°.

In the present work, we re-calculated vinyl (**1a**), formyl (**1b**), (*Z*)-imino (**1c**), and (*E*)-imino (**1d**) nitrileimines with the MP2/6-31+G(d), the MP2/6-311+G(d,p), and the B3LYP/6-311+G(d,p) levels of theory (Table 1). $H5_{in}$ and $H5_{out}$ represent an H5 atom located inside and outside of the molecule. The geometries of **1a** were bent forms in regard to the nitrileimine moiety with H1–C1–N2 angles of 135.9–144.0° and C1–N2–N3 angles of 170.6–170.8°. A vinyl group was almost planar with $H5_{in}$–C5–C4–N3 dihedral angles of −0.7 to −1.2° and $H5_{out}$–C5–C4–N3 dihedral angles of 178.6–178.9°. Geometries of **1b** were variable depending on basis sets and methods of electron correlation. Structures for

Table 1. Optimized Bond Lengths (Å), Bond Angles (°), and Dihedral Angles (°) of Conjugated Nitrileimines (**1a**–**1d**)

	1a			**1b**			**1c**			**1d**		
	I	II	III	I	II	III	I	II	III	I	II	III
C1–N2	1.192	1.189	1.186	1.178	1.175	1.155	1.189	1.186	1.175	1.184	1.181	1.164
N2–N3	1.262	1.255	1.241	1.277	1.269	1.270	1.263	1.256	1.249	1.270	1.263	1.259
N3–C4	1.411	1.409	1.408	1.400	1.402	1.396	1.419	1.417	1.416	1.399	1.399	1.396
C4–X5	1.347	1.347	1.338	1.228	1.216	1.212	1.284	1.281	1.270	1.288	1.284	1.275
C1–X5	3.491	3.467	3.571	3.343	3.345	3.402	3.514	3.491	3.573	3.323	3.320	3.398
H1–C1–N2	142.5	144.0	135.9	159.5	163.0	178.8	147.1	148.9	146.2	150.6	153.1	154.7
C1–N2–N3	170.6	170.8	170.8	174.2	174.6	175.9	172.2	172.5	172.8	172.1	172.4	173.2
N2–N3–C4	114.4	114.2	117.0	111.5	111.8	113.9	113.9	113.8	116.1	112.3	112.4	114.7
N3–C4–X5	127.3	127.1	127.8	126.5	126.5	126.9	130.3	130.1	130.5	123.4	123.5	124.3
H5$_{\text{in}}$–X5–C4	122.8	122.3	122.6	—	—	—	112.2	110.9	112.8	—	—	—
H5$_{\text{out}}$–X5–C4	119.7	119.5	119.9	—	—	—	—	—	—	109.9	108.9	110.6
H5$_{\text{in}}$–X5–H5$_{\text{out}}$	117.6	118.2	117.5	—	—	—	—	—	—	—	—	—
H1–C1–N2–N3	−151.8	−153.3	−147.4	−138.4	132.7	−0.8	−150.4	−152.2	−142.7	−148.2	−147.0	−135.6
C1–N2–N3–C4	−113.5	−111.7	−121.0	−125.8	130.4	−180.0	−110.4	−107.9	−122.5	−120.4	−121.4	−134.3
N2–N3–C4–X5	1.0	1.0	0.3	0.4	0.3	0.0	3.1	2.9	2.1	−0.9	−0.9	−1.2
H1–C1–N2-X5	99.8	99.8	96.4	98.5	99.2	179.2	104.6	105.0	99.4	94.4	94.5	92.3
H5$_{\text{in}}$–X5–C4–N3	−1.0	−1.2	−0.7	—	—	—	−0.7	−0.7	−0.5	—	—	—
H5$_{\text{out}}$–X5–C4–N3	178.7	178.6	178.9	—	—	—	—	—	—	179.3	179.2	179.6

I; MP2/6-31+G(d), II; MP2/6-311+G(d,p), III; B3LYP/6-311+G(d,p).

Table 2. Optimized Bond Lengths (Å), Bond Angles (°), and Dihedral Angles (°) of Heterocycles (**3a**–**3c**(**3d**))

	3a			**3b**			**3c**(**3d**)		
	I	II	III	I	II	III	I	II	III
C1–N2	1.299	1.296	1.282	1.303	1.300	1.286	1.323	1.320	1.300
N2–N3	1.450	1.440	1.440	1.400	1.390	1.400	1.380	1.370	1.380
N3–C4	1.290	1.290	1.280	1.300	1.290	1.280	1.320	1.320	1.300
C4–X5	1.490	1.490	1.490	1.360	1.350	1.350	1.360	1.360	1.360
C1–X5	1.490	1.490	1.490	1.360	1.350	1.350	1.360	1.360	1.360
H1–C1–N2	120.3	120.5	121.0	128.5	128.3	128.7	125.7	125.8	125.9
C1–N2–N3	107.9	108.1	108.3	105.7	105.7	105.9	107.2	107.3	107.4
N2–N3–C4	107.9	108.1	108.3	105.7	105.7	105.9	107.2	107.3	107.4
N3–C4–X5	113.1	112.9	112.8	113.5	113.5	113.2	110.3	110.3	110.3
H5–X5–C4	112.8	112.7	113.0	—	—	—	127.5	127.6	127.7
H5–X5–H5	107.4	107.9	107.0	—	—	—	—	—	—
H1–C1–N2–N3	180.0	180.0	180.0	180.0	180.0	180.0	180.0	180.0	180.0
C1–N2–N3–C4	0.0	0.0	0.0	0.0	0.0	0.0	0.0	0.0	0.0
N2–N3–C4–X5	0.0	0.0	0.0	0.0	0.0	0.0	0.0	0.0	0.0
H1–C1–N2–X5	180.0	180.0	180.0	180.0	180.0	180.0	180.0	180.0	180.0
H5–X5–C4–N3	119.0	118.7	119.2	—	—	—	180.0	180.0	180.0

I; MP2/6-31+G(d), II; MP2/6-311+G(d,p), III; B3LYP/6-311+G(d,p).

nitrileimine moiety of **1b** optimized at the MP2/6-31+G(d) level and the MP2/6-311+G(d,p) level were bent forms with H1–C1–N2 angles of 159.5–163.0° and C1–N2–N3 angles of 174.2–174.5°. A nitrileimine moiety of **1b** optimized at the B3LYP/6-311+G(d,p) level was almost linear with an H1–C1–N2 angle of 178.8° and a C1–N2–N3 angle of 175.9°. Geometries of **1c** and **1d** were close to those of **1a**. Nitrileimine moieties of **1c** and **1d** were essentially bent forms with H1–C1–N2 angles of 146.2–148.9° and 150.6–154.7° and C1–N2–N3 angles of 172.2–172.8° and 172.1–173.2°. The (*Z*)- and (*E*)-imino groups were almost planar with H5$_{\text{in}}$–N5–C4–N3 dihedral angles of −0.5 to −0.7° for **1c** and H5$_{\text{out}}$–N5–C4–N3 dihedral angles of 179.2–179.6° for **1d**.

Optimized geometries of the corresponding heterocycles **3a**–**3c**(**3d**) were completely planar with 0° and 180° of dihedral angles and had C_2 symmetry (Table 2).

All transition states (**2a**–**2d**) for the 1,5-electrocyclizations from **1** to **3** were located, and had single imaginary frequencies. Calculated energies for **2** and **3** relative to the corresponding nitrileimines (**1**) are shown in Table 3 and Fig. 4. This figure shows that the energies of **2** relative to **1** can be classified into two groups. The relative energies of **2a** and **2c** were substantially higher than those of **2b** and **2d**. The energies of **2** relative to **3**, which were activation energies in ring opening reactions from **3** to **1**, did not show such tendency (in square brackets in Table 3). Thus, it is expected that the cyclization processes from **1** to **2** will exhibit more remarkable pericyclic and pseudopericyclic characters compared with the ring open-

Table 3. Relative Energies (kcal mol^{-1})$^{a,b)}$ and Lowest Frequencies (cm^{-1}, in Parentheses) of Nitrileimines (**1a**–**1d**), Transition States (**2a**–**2d**), and Heterocycles (**3a**–**3c**(**3d**))

	I		II		III	
1a	0	(172.2)	0	(175.7)	0	(176.0)
2a	16.1	(497.3i)	15.8	(502.3i)	17.6	(487.8i)
	[59.9]		[58.1]		[54.6]	
3a	−43.8	(344.2)	−42.3	(323.0)	−37.0	(355.8)
1b	0	(168.8)	0	(166.8)	0	(170.0)
2b	9.12	(363.8i)	10.1	(389.6i)	8.46	(308.5i)
	[44.1]		[44.2]		[38.0]	
3b	−34.9	(639.3)	−34.1	(639.8)	−29.5	(640.9)
1c	0	(170.2)	0	(170.2)	0	(174.5)
2c	19.0	(628.5i)	18.4	(614.4i)	18.9	(577.6i)
	[79.0]		[76.7]		[71.7]	
3c(**3d**)	−60.0	(509.8)	−58.3	(512.5)	−52.8	(531.2)
1d	0	(176.3)	0	(172.7)	0	(174.5)
2d	7.49	(357.3i)	7.85	(372.7i)	6.87	(316.8i)
	[64.9]		[63.7]		[57.3]	
3c(**3d**)	−57.4	(509.8)	−55.8	(512.5)	−50.4	(531.2)

a) Energies, which include zero point energy (ZPE) without scaling, are relative to nitrileimines (**1**). b) Energies of transition states (**2**) relative to those of heterocycles (**3**) are in square brackets. I; MP2/6-31+G(d)//MP2/6-31+G(d), II; MP2/6-311+G(d,p)//MP2/6-311+G(d,p), III; B3LYP/6-311+G(d,p)//B3LYP/6-311+G(d,p).

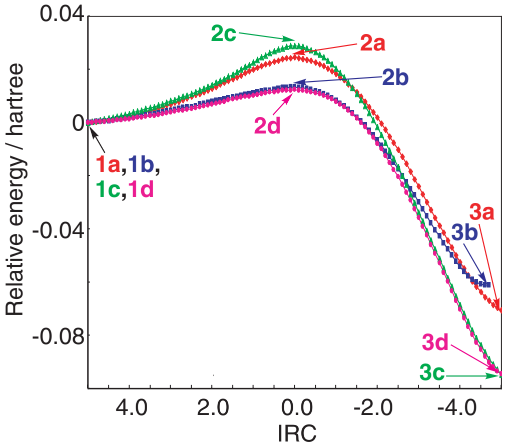

Fig. 4. Relative energies, which do not include zero-point vibration energy, calculated at the MP2/6-31+G(d)//MP2/6-31+G(d) level of theory along IRC from nitrileimines (**1**) to heterocycles (**3**).

ing processes from **3** to **2**.

Optimized geometries of the transition states **2a**–**2d** are illustrated in Fig. 5. In the geometries of nitrileimine moieties, C1–N2–N3 angles decreased at all transition states (**2a**–**2d**) by 28.4–43.4° as the ring closures proceeded. In geometries of conjugated groups, a C4–C5 bond of **2a** and a C4–N5 bond of **2c** were apparently twisted with dihedral angles of −39.4 to −41.8° for $\mathrm{H5_{in}}$–C5–C4–N3 and dihedral angles of 159.7–160.3° for $\mathrm{H5_{out}}$–C5–C4–N3 for **2a**, and dihedral angles of −41.4 to −44.2° for $\mathrm{H5_{in}}$–N5–C4–N3 for **2c**. The H1–C1 bonds were tilted toward the outsides of the molecules by twisting of C1–N2 bonds with increasing H1–C1–N2–N3 dihedral angles compared to **1a** and **1c**. The twisting in C1–N2 bonds and C4–X5 bonds suggests that the reactions proceeded in disrotatory modes. In **2b** and **2d**, H1–C1–N2 angles were larger than those of **2a** and **2c**, which indicated that the H1–C1–N2 moieties are more linear and C1 has more sp character in **2b** and **2d**. Differences in C1–N2 bond lengths between **2b** and **2d** (1.178–1.192 Å) and **2a** and **2c** (1.221–1.228 Å) were also in agreement with the increased sp character in **2b** and **2d**. Thus, no twisting around C1–N2 bonds is apparent, as seen in **2a** and **2c**. Twisting of a C4–N5 bond in the reaction from **1d** to **2d** was negligible, because the change in an $\mathrm{H5_{out}}$–N5–C4–N3 dihedral angle was 3.4° at most. The planarity of the (*E*)-imino group was maintained in the pathway from **1d** to **2d**. At the transition state of the formyl derivative (**2b**), the geometry of the whole molecule was completely planar, although there was no substituent that can be a structural probe for twisting of the formyl group. The planarity observed at **2d** and **2b** seems to indicate that the reactions have some pseudopericyclic natures.

NBO analysis along IRC. Stereochemical features at the transition states (**2a**–**2d**) and energy barriers of the reactions indicated that the 1,5-electrocyclizations of **1a** and **1c** were pericyclic reactions, and those of **1b** and **1d** seemed to have pseudopericyclic natures. In order to confirm the classification of the reactions, we have carried out the NBO analysis along IRC of the reactions. Names of the orbitals are defined as illustrated in Fig. 6. Here we denote π-orbitals and lone pair electrons as π and n. Suffixes (v) and (h) are used to represent *vertical* and *horizontal* in regard to the mean molecular plane. Occupancies of selected localized bonding and nonbonding orbitals are listed in Table 4, and results of the second order perturbation theory analysis of NBO basis[19] along IRC from nitrileimines (**1**) to heterocycles (**3**) are summarized in Figs. 7–10 and Table 5.

The NBO analysis of **1a**–**1d** indicated that the C1–N2 bonds had a triple bond character, regardless of whether the geometries of the nitrileimine moieties were bent forms or a linear

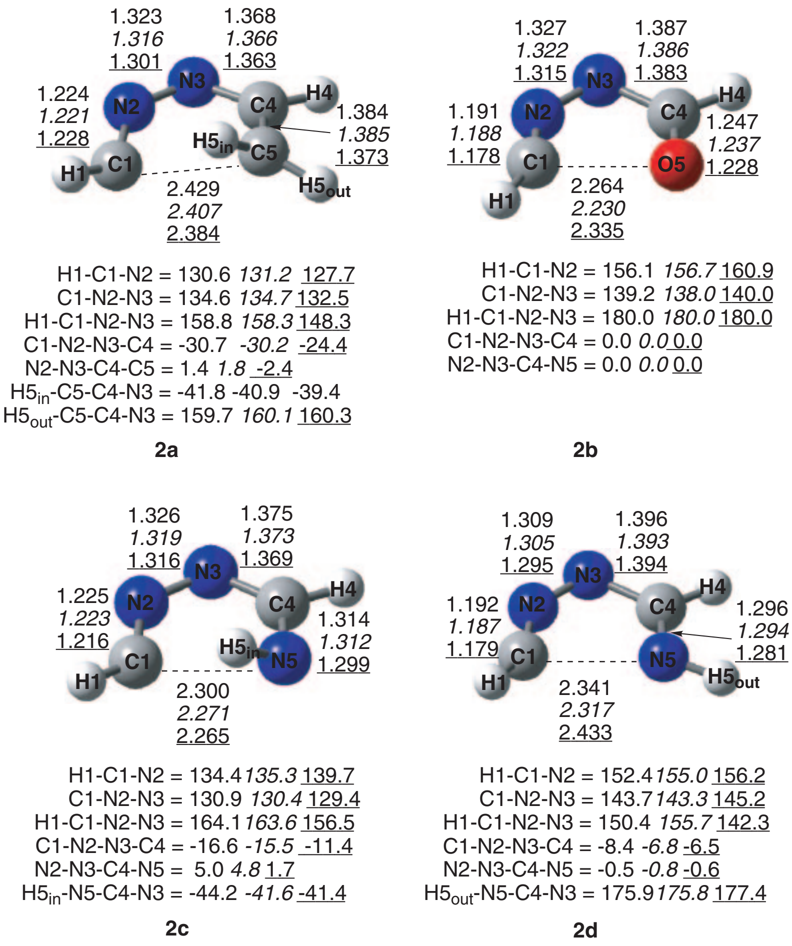

Fig. 5. Structures of transition states (**2a**–**2d**) for 1,5-electrocyclization of conjugated nitrileimines optimized at the MP2/6-311+G(d,p)//MP2/6-311+G(d,p) level of theory, and selected bond lengths (Å), bond angles (°), and dihedral angles (°) of **2a**–**2d** obtained at the MP2/6-31+G(d)//MP2/6-31+G(d), MP2/6-311+G(d,p)//MP2/6-311+G(d,p) (italic), and the B3LYP/6-311+G(d,p)//B3LYP/6-311+G(d,p) (underline) levels of theory.

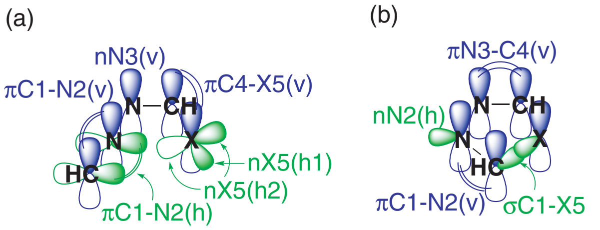

Fig. 6. Natural bond orbitals (NBOs); (a) from nitrileimines (**1**) to transition states (**2**), and (b) from transition states (**2**) to heterocycles (**3**).

form. Lone pair electrons nN3(v) were delocalized over πC1–N2(v) and πC4–X5(v).

In the pathway from **1a** to **2a**, occupancies of πC4–C5(v) and nN3(v) decreased as the reaction proceeds (Table 4). The second order perturbation analysis along IRC (Fig. 7) shows that the decrease in occupancy of πC4–C5(v) was mainly due to remote electron-donation to an antibonding π^*C1–N2(h) orbital, which was increasing near **2a**. At 2.5 in IRC, the second order energy-lowering of πC4–C5(v)/π^*C1–N2(h) (Fig. 7, V) is 0.55 kcal mol^{-1}, where $\Delta E_{i,j} =$ 0.57 au and $F_{i,j} = 0.016$ au (Table 5). The energy-lowering increased as the reaction proceeded, and became 14.06 kcal mol^{-1} at **2a**, where $\Delta E_{i,j} = 0.38$ au and $F_{i,j} = 0.078$ au. In this process, the difference in energy of the orbitals ($\Delta E_{i,j}$) varied as the geometry of the molecule changed, and element of the Fock matrix ($F_{i,j}$) increased with increment of overlap between the orbitals. The changes in $\Delta E_{i,j}$ and $F_{i,j}$ indicate that the π-orbitals in the whole molecule including πC4–C5(v) and π^*C1–N2(h) interact cooperatively in the process from **1a** to **2a**. The decrease in occupancy of nN3(v) was mainly due to electron-donation to adjacent antibonding π^*C1–N2(h) (Fig. 7, II) and π^*C4–C5(v) (Fig. 7, III) orbitals. The major accepting orbitals were changed from π^*C1–N2(v) (Fig. 7, I) at the early stage of the reaction to π^*C1–N2(h) near the transition state (**2a**), which indicates that the 1,3-dipole moiety was twisted during the pathway from **1a** to **2a**.

In the pathway from **2a** to **3a**, there were electron-donating interactions between the forming C1–C5 bond and the other π-orbitals, such as from σC1–C5 to π^*N3–C4(v) (Fig. 7, VI), from πN3–C4(v) to σ^*C1–C5 (Fig. 7, VII), and from nN2(h) to σ^*C1–C5 (Fig. 7, XI), just after passing TS(**2a**). These interactions, which weaken a σC1–C5 bond, were re-

Table 4. Selected Occupancy of NBO Basis for 1,5-Electrocyclization of **1** and **2** Calculated at the MP2/6-31+G(d)//MP2/6-31+G(d) Level of Theory

	πC1–N2(h)	πC1–N2(v)	nN3(v)	πC4–C5(v)	nX5
1a	1.986	1.983	1.439	1.974	—
2a	1.936	1.966	1.292	1.791	—
Δ(**2a** − **1a**)[a]	(−0.058)	(−0.017)	(−0.147)	(−0.183)	
1b	1.989	1.987	1.550	1.995	1.901
2b	1.978	1.988	1.529	1.992	1.837
Δ(**2b** − **1b**)[a]	(−0.011)	(0.001)	(−0.021)	(−0.003)	(−0.064)
1c	1.985	1.985	1.486	1.987	1.946
2c	1.974	1.973	1.397	1.852	1.909
Δ(**2c** − **1c**)[a]	(−0.011)	(−0.012)	(−0.089)	(−0.135)	(−0.037)
1d	1.980	1.978	1.516	1.989	1.952
2d	1.957	1.952	1.514	1.984	1.885
Δ(**2d** − **1d**)[a]	(−0.023)	(−0.026)	(−0.002)	(−0.005)	(−0.067)

a) Difference in occupancies between nitrileimines (**1**) and transition states (**2**).

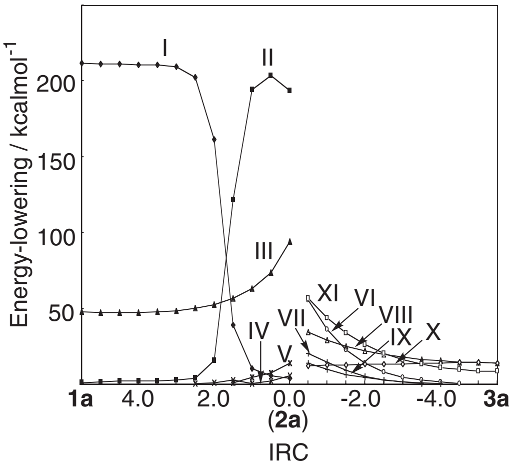

Fig. 7. The second order perturbative energy-lowering between selected donor/acceptor orbitals along IRC of the reaction from **1a** to **3a**. I, nN3(v)/π^*C1–N2(v); II, nN3(v)/π^*C1–N2(h); III, nN3(v)/π^*C4–C5(v); IV, πC4–C5(v)/π^*C1–N2(v); V, πC4–C5(v)/π^*C1–N2(h); VI, σC1–C5/π^*N3–C4(v); VII, πN3–C4(v)/σ^*C1–C5; VIII, πN3–C4(v)/π^*C1–N2(v); IX, πC1–N2(v)/σ^*C1–C5; X, πC1–N2(v)/π^*N3–C4(v); XI, nN2(h)/σ^*C1–C5.

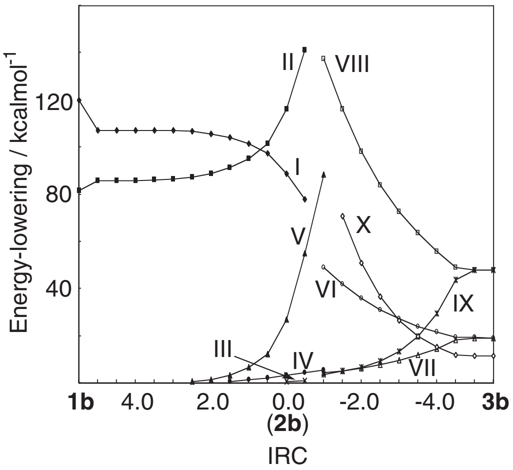

Fig. 8. The second order perturbative energy-lowering between selected donor/acceptor orbitals along IRC of the reaction from **1b** to **3b**. I, nN3(v)/π^*C1–N2(v); II, nN3(v)/π^*C4–O5(v); III, πC4–O5(v)/π^*C1–N2(v); IV, nO5(h1)/π^*C1–N2(h); V, nO5(h2)/π^*C1–N2(h); VI, πN3–C4(v)/π^*C1–N2(v); VII, πC1–N2(v)/π^*N3–C4(v); VIII, nO5(v)/π^*N3–C4(v); IX, nO5(v)/π^*C1–N2(v); X, nN2(h)/σ^*C1–O5.

duced as the reaction proceeded. In other words, in the reverse (ring-opening) process from **3a** to **1a**, these interactions play important roles in breaking the C1–C5 bond near the transition state (**2a**).

Electronic features of the reaction from **1b** to **2b** were in sharp contrast to those of **1a** to **2a** (Table 4 and Fig. 8). Changes in occupancies of NBOs from **1b** to **2b** were relatively small compared with those from **1a** to **2a**, except for decrease in occupancy of nO5(h2). Interaction between πC4–O5(v) and π^*C1–N2(v) was negligible throughout the reaction. Instead, electron-donation from nO5(h2) to π^*C1–N2(h) (Fig. 8, V) was significant (88.25 kcal mol^{-1}) around **2b**, which led to a σC1–O5 bond formation. The $F_{i,j}$ of the interaction between nO5(h2) and π^*C1–N2(h) increased from 0.018 au to 0.208 au at 2.5 and −1.0 in the IRC, which indicates increasing overlap of the orbitals, while the $\Delta E_{i,j}$ was kept constant (0.62 au to 0.60 au) (Table 5). This behavior can be interpreted as meaning that the nO5(h2) and the π^*C1–N2(h) orbitals are electronically isolated from the other π-orbitals, and thus the $\Delta E_{i,j}$ is insensitive to changes in the other part of the molecule. There were electron-donations from nN3(v) to adjacent π^*C1–N2(v) (Fig. 8, I) and π^*C4–O5(v) (Fig. 8, II), while donation to π^*C1–N2(h) was negligible. This indicated the nitrileimine moiety did not twist during the pathway from **1b** to **2b**.

In the pathway from **2b** to **3b**, there were electron-donating interactions from nO5(v) to π^*N3–C4(v) (Fig. 8, VIII), from πN3–C4(v) to π^*C1–N2(v) (Fig. 8, VI), and from nN2(h) to σ^*C1–O5 (Fig. 8, X), just after passing TS (**2b**). The last one weakened a σC1–O5 bond, and was gradually reduced as the reaction proceeded. In the reverse (ring-opening) process from **3b** to **2b**, the electron donation from nN2(h) to

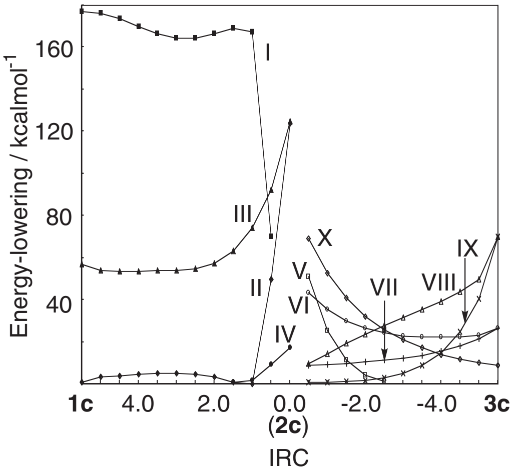

Fig. 9. The second order perturbative energy-lowering between selected donor/acceptor orbitals along IRC of the reaction from **1c** to **3c**. I, nN3(v)/π*C1–N2(v); II, nN3(v)/π*C1–N2(h); III, nN3(v)/π*C4–N5(v); IV, πC4–N5(v)/π*C1–N2(v); V, σC1–N5/π*N3–C4(v); VI, πN3–C4(v)/π*C1–N2(v); VII, πC1–N2(v)/π*N3–C4(v); VIII, nN5(v)/π*N3–C4(v); IX, nN5(v)/π*C1–N2(v); X, nN2(h)/σ*C1–N5.

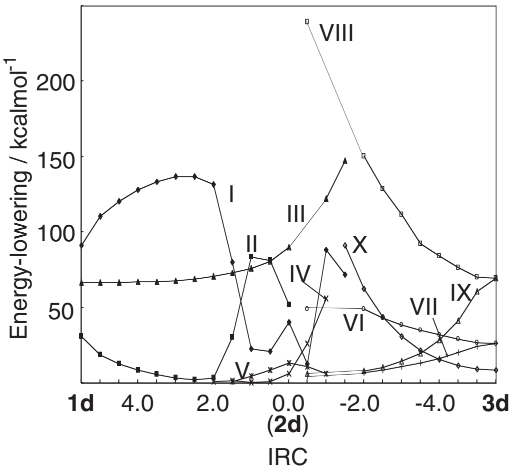

Fig. 10. The second order perturbative energy-lowering between selected donor/acceptor orbitals along IRC of the reaction from **1d** to **3d**. I, nN3(v)/π*C1–N2(v); II, nN3(v)/π*C1–N2(h); III, nN3(v)/π*C4–N5(v); IV, nN5(h)/π*C1–N2(h); V, nN5(h)/π*C1–N2(v); VI, πN3–C4(v)/π*C1–N2(v); VII, πC1–N2(v)/π*N3–C4(v); VIII, nN5(v)/π*N3–C4(v); IX, nN5(v)/π*C1–N2(v); X, nN2(h)/σ*C1–N5.

Table 5. Second Order Energy-Lowering by Perturbative Donor/Acceptor Interaction for C1–X5 Bond Formation Along IRC Calculated at the MP2/6-31+G(d)//MP2/6-31+G(d) Level of Theory[a)]

IRC	Donor NBO/Acceptor NBO								
	πC4–C5(v) /π*C1–N2(v) (from **1a** to **2a**)			πC4–C5(v) /π*C1–N2(h) (from **1a** to **2a**)			nO5(h2) /π*C1–N2(h) (from **1b** to **3b**)		
	$\Delta E_{i,j}^{(2)\mathrm{b)}}$	$\Delta E_{i,j}^{\mathrm{c)}}$	$F_{i,j}^{\mathrm{d)}}$	$\Delta E_{i,j}^{(2)\mathrm{b)}}$	$\Delta E_{i,j}^{\mathrm{c)}}$	$F_{i,j}^{\mathrm{d)}}$	$\Delta E_{i,j}^{(2)\mathrm{b)}}$	$\Delta E_{i,j}^{\mathrm{c)}}$	$F_{i,j}^{\mathrm{d)}}$
2.5				0.55	0.57	0.016	0.66	0.62	0.018
2.0				1.42	0.54	0.026	1.68	0.62	0.029
1.5				3.08	0.45	0.037	3.55	0.62	0.042
1.0	0.83	0.56	0.019	4.49	0.42	0.044	6.86	0.62	0.058
0.5	2.37	0.56	0.033	7.39	0.40	0.056	12.53	0.62	0.079
0 (**2**)	5.80	0.53	0.051	14.06	0.38	0.074	27.16	0.62	0.117
−0.5							55.16	0.62	0.167
−1.0							88.25	0.60	0.208

IRC	Donor NBO/Acceptor NBO											
	πC4–N5(v) /π*C1–N2(v) (from **1c** to **2c**)			πC4–N5(v) /π*C1–N2(h) (from **1c** to **2c**)			nN5(h) /π*C1–N2(v) (from **1d** to **2d**)			nN5(h) /π*C1–N2(h) (from **1d** to **2d**)		
	$\Delta E_{i,j}^{(2)\mathrm{b)}}$	$\Delta E_{i,j}^{\mathrm{c)}}$	$F_{i,j}^{\mathrm{d)}}$	$\Delta E_{i,j}^{(2)\mathrm{b)}}$	$\Delta E_{i,j}^{\mathrm{c)}}$	$F_{i,j}^{\mathrm{d)}}$	$\Delta E_{i,j}^{(2)\mathrm{b)}}$	$\Delta E_{i,j}^{\mathrm{c)}}$	$F_{i,j}^{\mathrm{d)}}$	$\Delta E_{i,j}^{(2)\mathrm{b)}}$	$\Delta E_{i,j}^{\mathrm{c)}}$	$F_{i,j}^{\mathrm{d)}}$
2.0				0.55	1.29	0.029				1.20	0.78	0.027
1.5	0.77	0.55	0.020	1.12	0.60	0.024	1.15	0.72	0.027	1.48	0.76	0.031
1.0	1.84	0.54	0.031	2.10	0.59	0.032	4.94	0.74	0.055	0.72	0.74	0.022
0.5	9.32	0.49	0.066				8.96	0.74	0.074	1.39	0.74	0.030
0 (**2**)	17.25	0.53	0.087	4.90	0.53	0.048	13.60	0.71	0.091	6.23	0.74	0.062

a) A blank means energy is lower than 0.5 kcal mol^{-1}. b) The second order energy-lowering by perturbative interaction between ϕ_i and ϕ_j (kcal mol^{-1}).[19] c) Energy-difference between NBOs ϕ_i and ϕ_j (hartree). c) Fock matrix element (hartree).

σ*C1–O5 orbital plays a major role in breaking the C1–O5 bond near the transition state. As the ring opening proceeded, symmetry in the geometry of **3b** was lost. Electron-donating interactions from nO5(v) to π*N3–C4(v) and π*C1–N2(v) (Fig. 8, IX) are the same in **3b**. Then the former became larger and the latter became smaller as the ring opening reaction proceeded from **3b** to **2b**. Similar breaking of symmetry is occurring in the electron-donating interactions from πN3–C4(v) to π*C1–N2(v) and from πC1–N2(v) to π*N3–C4(v) (Fig. 8, VII).

Electronic features along pathway from **1c** to **2c** showed that the reaction has some characteristics of the pericyclic reaction similar to the reaction from **1a** to **2a**. Occupancy of πC4–N5(v) decreased as the reaction proceeded (Table 4), which was explained by increasing electron-donation to π^*C1–N2(v) (Fig. 9, IV). The major accepting orbital for electron-donation from nN3(v) was π^*C1–N2(v) (Fig. 9, I) in the early stage of the reaction, and then changed to π^*C1–N2(h) (Fig. 9, II), indicating that the nitrileimine moiety was twisted near the transition state (**2c**). There were electron-donations from σC1–N5 to π^*N3–C4(v) (Fig. 9, V) and from nN2(h) to σ^*C1–N5 (Fig. 9, X) just after passing **2c**. These interactions play important roles in the ring opening process from **3c** to **2c**.

In the pathway from **1d** to **2d**, occupancy of nN5(h) decreased as the reaction proceeded (Table 4). The decrease in occupancy was caused by the remote electron-donations from nN5(h) to π^*C1–N2(h) (Fig. 10, II) and π^*C1–N2(v) (Fig. 10, I). The $F_{i,j}$ for the nN5(h)/π^*C1–N2(h) interaction increased from 0.027 au at 2.0 in IRC to 0.062 au at **2d**, while $\Delta E_{i,j}$ was almost constant (0.78 au to 0.74 au) (Table 5). The $F_{i,j}$ for the nN5(h)/π^*C1–N2(v) interaction also increased from 0.027 au at 1.5 in IRC to 0.091 au at **2d**, while $\Delta E_{i,j}$ was almost constant (0.74 au to 0.71 au). These interactions led to new bond formation between C1 and N5, while the contribution of πC4–N5(v) orbital was negligible. The interaction between nN3(v) and π^*C1–N2(h) was smaller than that between nN3(v) and π^*C1–N2(v) at the beginning of the reaction. Then, the former interaction became stronger than the latter near **2d**, which indicated that the nitrileimine moiety was twisted as the reaction proceeded.

Figure 11 illustrates a summary of the donor/acceptor interactions based on the second order perturbation analysis of the NBOs at the transition states. At **2a** and **2c**, there are cyclic interactions of the orbitals around the molecules. On the other hand, at **2b**, there are two disconnections at C1 and O5 in the sense of non-covalent donor/acceptor orbital interactions. At **2d**, the orbital interaction has a single disconnection at N5. There is no disconnection at C1 in **2d**, since the twisting in the nitrileimine moiety caused doubly degenerated interactions between C1 and N5.

Mechanisms of the 1,5-Electrocyclizations. The cyclizations of vinyl nitrileimine (**1a**) and (*Z*)-imino nitrileimine (**1c**) are typical pericyclic 6π-electrocyclizations. The interactions of π-orbitals between C1 and X5 increase as the reactions proceed, and result in formations of C1–X5 bonds. Such interactions are accompanied by the interactions of π-orbitals on the other part of the molecules. The electrons at the forming σC1–X5 bonds, which project out of the mean molecular plane, interact with π^*N3–C4(v) orbital near the transition states (**2a**, **2c**).

The 1,5-cyclization of formyl nitrileimine (**1b**) is considered to be a pseudopericyclic reaction. The mechanism has been identified based on electronic features, since there is no decisive stereochemical feature. During the path from **1b** to **2b**, the interaction between lone pair electrons at O5 and horizontal antibonding π^*C1–N2(h) orbital leads to a bond formation between C1 and O5, while interaction between vertical π- and π^*-orbitals at both ends of the molecule is negligible. There is no interaction between vertical π-orbitals and the forming σC1–O5 bond because of their orthogonal array. Thus, there are two disconnections for the interactions of the orbitals at C1 and N5. The low energy barrier and the perfect planer geometry of **2b** are also consistent with a pseudopericyclic reaction.

The 1,5-cyclization of (*E*)-imino nitrileimine (**1d**) showed some typical features for a pseudopericyclic reaction. The reaction has a low energy barrier that is close to that of the reaction of **1b**. Contribution of πC4–N5(v) electrons to the bond formation between C1 and N5 is negligible compared with nucleophilic interactions of nN5. However, some stereochemical and electronic features show that the reaction of **1d** is not a typical pseudopericyclic reaction. The planarity of the transition state (**2d**) is not perfect. Both the π^*C1–N2(h) and π^*C1–N2(v) orbitals accept electron donation from nN3(v) and nN5(h), because of twisting in the nitrileimine moiety. Thus, there is a single disconnection of the interactions of the orbitals at N5.[20] Taking these factors into consideration, the reaction of **1d** has a pseudopericyclic nature to some extent, though it is incomplete.

Conclusion

We have applied the NBO analyses along IRC, including analyses of occupancy and the second order perturbative energy-lowering, to classification of mechanisms for the 1,5-electrocyclizations of the conjugated nitrileimines. The analyses have indicated that there are three types of mechanisms. The reactions of vinyl nitrileimine (**1a**) and (*Z*)-imino nitrileimine (**1c**) are pericyclic reactions. The reaction of formyl nitrileimine (**1b**) is a typical pseudopericyclic reaction, which has two disconnections of orbital-interactions. The 1,5-electrocyclizations of (*E*)-imino nitrileimine (**1d**) is an incomplete pseu-

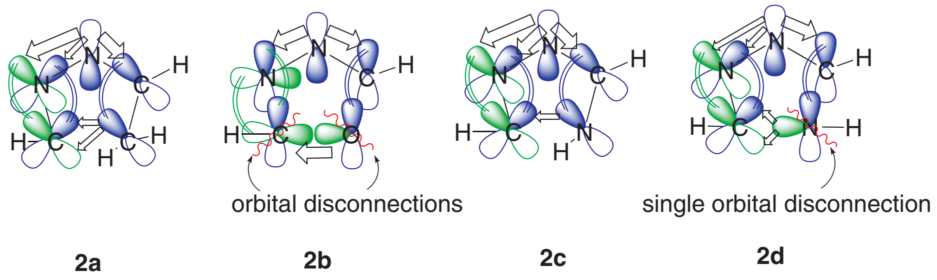

Fig. 11. Schematic representation of interactions between orbitals at the transition states (**2a**–**2d**) based on the second order perturbation analysis of donor/acceptor NBOs.

dopericyclic reaction, which has a single disconnection of orbital-interactions.

References

1 J. A. Ross, R. P. Seiders, and D. M. Lemal, *J. Am. Chem. Soc.*, **98**, 4325 (1976).

2 a) D. M. Birney and P. E. Wagenseller, *J. Am. Chem. Soc.*, **116**, 6262 (1994). b) D. M. Birney, S. Ham, and G. R. Unruh, *J. Am. Chem. Soc.*, **119**, 4509 (1997). c) D. M. Birney, X. Xu, and S. Ham, *Angew. Chem., Int. Ed.*, **38**, 189 (1999).

3 a) L. A. Burke, J. Elguero, G. Leroy, and M. Sana, *J. Am. Chem. Soc.*, **98**, 1685 (1976). b) L. A. Burke, G. Leroy, M. T. Nguyen, and M. Sana, *J. Am. Chem. Soc.*, **100**, 3668 (1978).

4 a) V. A. Bakulev and P. Gloriozov, *Khim. Geterotsikl. Soedin.*, **1989**, 504. b) V. A. Bakulev, Y. Yu. Morzherin, A. T. Lebedev, E. F. Dankova, M. Yu. Kolobov, and Y. M. Shafran, *Bull. Soc. Chim. Belg.*, **102**, 493 (1993). c) W. M. F. Fabian, V. A. Bakulev, and C. O. Kappe, *J. Org. Chem.*, **63**, 5801 (1998).

5 W. M. F. Fabian, C. O. Kappe, and V. A. Bakulev, *J. Org. Chem.*, **65**, 47 (2000).

6 E. M. Cabaleiro-Lago, J. Rodriguez-Otero, and J. M. Hermida-Ramon, *J. Phys. Chem. A*, **107**, 4962 (2003).

7 a) K. Fukushima, Y.-Q. Lu, and T. Ibata, *Bull. Chem. Soc. Jpn.*, **69**, 3289 (1996). b) K. Fukushima, *Bull. Wakayama Med. College (Liberal Arts and Sciences)*, **29**, 61 (1999). c) K. Fukushima, *Bull. Wakayama Med. Univ. (Liberal Arts and Sciences)*, **31**, 17 (2001). d) K. Fukushima, *Bull. Wakayama Med. Univ. (Liberal Arts and Sciences)*, **32**, 25 (2002).

8 a) A. R. de Lera, R. Alvarez, B. Lecea, A. Torrado, and F. P. Cossio, *Angew. Chem., Int. Ed.*, **40**, 557 (2001). b) J. Rodriguez-Otero and E. M. Cabaleiro-Lago, *Angew. Chem., Int. Ed.*, **41**, 1147 (2002). c) A. R. de Lera and F. P. Cossio, *Angew. Chem., Int. Ed.*, **41**, 1150 (2002). d) J. Rodriguez-Otero and E. M. Cabaleiro-Lago, *Chem.—Eur. J.*, **9**, 1837 (2003).

9 a) E. C. Taylor and I. J. Turchi, *Chem. Rev.*, **79**, 181 (1979). b) R. Huisgen, *Angew. Chem., Int. Ed. Engl.*, **19**, 947 (1980).

10 a) R. Huisgen, J. Sauer, H. J. Sturm, and J. H. Markgraf, *Chem. Ber.*, **93**, 2106 (1960). b) R. Huisgen, J. Sauer, and M. Seidel, *Chem. Ber.*, **93**, 2885 (1960). c) R. Huisgen, H. J. Sturm, and M. Seidel, *Chem. Ber.*, **94**, 1555 (1961). d) R. Huisgen, C. Axen, and H. Seidel, *Chem. Ber.*, **98**, 2966 (1965).

11 A. Konnecke, R. Dorre, and E. Lippmann, *Tetrahedron Lett.*, **19**, 2071 (1978).

12 P. Caramella and K. N. Houk, *J. Am. Chem. Soc.*, **98**, 6397 (1976).

13 K. Fukushima, *Bull. Wakayama Med. Univ. (Liberal Arts and Sciences)*, **30**, 25 (2000).

14 M. J. Frisch, G. W. Trucks, H. B. Schlegel, G. E. Scuseria, M. A. Robb, J. R. Cheeseman, V. G. Zakrzewski, J. A. Montgomery, Jr., R. E. Stratmann, J. C. Burant, S. Dapprich, J. M. Millam, A. D. Daniels, K. N. Kudin, M. C. Strain, O. Farkas, J. Tomasi, V. Barone, M. Cossi, R. Cammi, B. Mennucci, C. Pomelli, C. Adamo, S. Clifford, J. Ochterski, G. A. Petersson, P. Y. Ayala, Q. Cui, K. Morokuma, P. Salvador, J. J. Dannenberg, D. K. Malick, A. D. Rabuck, K. Raghavachari, J. B. Foresman, J. Cioslowski, J. V. Ortiz, A. G. Baboul, B. B. Stefanov, G. Liu, A. Liashenko, P. Piskorz, I. Komaromi, R. Gomperts, R. L. Martin, D. J. Fox, T. Keith, M. A. Al-Laham, C. Y. Peng, A. Nanayakkara, M. Challacombe, P. M. W. Gill, B. Johnson, W. Chen, M. W. Wong, J. L. Andres, C. Gonzalez, M. Head-Gordon, E. S. Replogle, and J. A. Pople, "Gaussian 98, Revision A.11," Gaussian, Inc., Pittsburgh PA, 2001.

15 M. Head-Gordon, J. A. Pople, and M. J. Frisch, *Chem. Phys. Lett.*, **153**, 503 (1988).

16 A. D. Becke, *J. Chem. Phys.*, **98**, 5648 (1993).

17 a) NBO Version 3.1, E. D. Glendening, A. E. Reed, J. E. Carpenter, and F. Weinhold. b) A. E. Reed, L. A. Curtiss, and F. Weinhold, *Chem. Rev.*, **88**, 899 (1988).

18 C. Gonzalez and H. B. Schlegel, *J. Chem. Phys.*, **90**, 2154 (1989).

19 The stabilized energy by the second order perturbation between localized orbitals ϕ_i and ϕ_j ($\Delta E_{i,j}{}^{(2)}$) is obtained by the following equation.[17b]

$$\Delta E_{i,j}{}^{(2)} = -2(F_{i,j})^2/\Delta E_{i,j} \tag{1}$$

where $F_{i,j}$ is element of the Fock matrix,

$$F_{i,j} = \langle \phi_i | \mathbf{F} | \phi_j \rangle \tag{2}$$

where **F** is the Fock operator.

$F_{i,j}$ represents interaction between ϕ_i and ϕ_j, and $\Delta E_{i,j}$ is difference in energy between ϕ_i and ϕ_j.

20 Pericyclic and pseudopericyclic reactions which has a single disconnection of orbital interactions were discussed in some cheletropic reactions.[2b] In these reactions, a CO group extruded with breaking of two σ-bonds in one step. If the orbital disconnection was at the stronger-interacting site, the reaction has more pseudopericyclic character. However, the results in the cheletropic reactions are not directly applicable to the 1,5-electrocyclization of **1d**, since the reaction of **1d** includes formation of one σ-bond.